UC Davis
UC Davis Previously Published Works

Title

An atlas of small RNAs from potato.

Permalink

https://escholarship.org/uc/item/192610pm

Journal

Plant Direct, 6(12)

Authors

Baldrich, Patricia

Liu, Alexander

Meyers, Blake

et al.

Publication Date

2022-12-01

DOI

10.1002/pld3.466

Copyright Information

Peer reviewed

ORIGINAL RESEARCH

An atlas of small RNAs from potato

Patricia Baldrich[1] | Alexander Liu[1] | Blake C. Meyers[1,2] |
Vincent N. Fondong[3]

[1]Donald Danforth Plant Science Center, St. Louis, Missouri, USA

[2]Division of Plant Science & Technology, University of Missouri-Columbia, Columbia, Missouri, USA

[3]Department of Biological Sciences, Delaware State University, Dover, Delaware, USA

Correspondence
Patricia Baldrich, Donald Danforth Plant Science Center, St. Louis, MO 63132, USA.
Email: pbaldrich@danforthcenter.org

Abstract

Small RNAs, including microRNAs (miRNAs), phased secondary small interfering RNAs (phasiRNA), and heterochromatic small interfering RNAs (hc-siRNA) are an essential component of gene regulation. To establish a broad potato small RNA atlas, we constructed an expression atlas of leaves, flowers, roots, and tubers of Desiree and Eva, which are commercially important potato (*Solanum tuberosum*) cultivars. All small RNAs identified were observed to be conserved between both cultivars, supporting the hypothesis that small RNAs have a low evolutionary rate and are mostly conserved between lineages. However, we also found that a few miRNAs showed differential accumulation between the two potato cultivars, and that hc-siRNAs have a tissue specific expression. We further identified dozens of reproductive and non-reproductive phasiRNAs originating from coding and noncoding regions that appeared to exhibit tissue-specific expression. Together, this study provides an extensive small RNA profiling of different potato tissues that might be used as a resource for future investigations.

KEYWORDS
hc-siRNA, miRNAs, phasiRNAs, potato, small RNAs

1 | INTRODUCTION

Potato (*Solanum tuberosum L.*) is the third largest food crop in the world (Tiwari et al., 2022). It belongs to the *Solanaceae* family and is native to the Andes region in South America, where it was first domesticated. Potato grows as an herbaceous multi-stemmed plant and bears pinnate leaves. Flowers emerge in the summer and may display white, pink, blue, or purple color with yellow stamens. When produced, potato fruits display a green color with cherry tomato-like berries filled with many seeds. Potatoes are cultivated for their tubers, which are enlarged, underground stems that function as storage organs for starch and other nutrients. Most cultivated potatoes are autotetraploid (2n = 4x = 48), although their ploidy can vary from diploid to pentaploid (Machida-Hirano, 2015). There are also wild potato species that are hexaploid (Watanabe, 2015). Due to their complex genetics, potatoes are clonally propagated through tubers and through tissue culture. The potato plant is morphologically diverse, with thousands of cultivated varieties (or cultivars) and landraces. However, a much lower diversity is found in commercially produced potatoes. In this work, we focused on two cultivars, namely Desiree and Eva that were developed in the Netherlands and the United States, respectively (Figure S1). Tubers of Desiree have yellow flesh and red skin. Desiree is valued for its resistance to drought and moderate resistance to diseases (Jones & Vincent, 2018). The Eva cultivar was selected from a cross between the Stuben cultivar and bulk pollen collected from clones that were neotuberosum × tuberosum hybrids (Plaisted et al., 2001). This cultivar has white flesh and skin and is appreciated for its well-shaped and uniform tubers. Eva is

---

Patricia Baldrich and Alexander Liu contributed equally to this work.

extremely resistant to diseases, including especially potato virus Y and potato virus X.

As a result of the many challenges associated with conventional breeding for potato improvement, alternative strategies are required to manage the constraints faced in the cultivation of this crop. The use of genetic engineering in potato improvement is likely to make considerable strides thanks to advances in genomics and genomics technologies. Thus, in the last decade, several potato reference genomes have been sequenced, including the doubled monoploid *Solanum tuberosum* Group phureja DM1–3 (Xu et al., 2011), the wild diploid *S. commersonii* (Aversano et al., 2015), and the diploid, inbred clone of *Solanum chacoense* - M6 (Leisner et al., 2018). Given that potato is an autotetraploid, it has been suggested that its polyploid nature resulted from duplication events (Kyriakidou et al., 2020). Thus, to capture the diversity exhibited by diverse potato genomes, different sequencing technologies are fundamental, and will lead to a better understanding of the potato genome.

The availability of potato whole genome sequences has allowed parallel sequencing and identification of small RNAs (sRNAs), which are a critical part of the regulation of many cellular functions and development (Baldrich et al., 2019; Samad et al., 2017). Plant sRNAs are between 21 and 24 nt in length and, depending on their biogenesis, can be divided into three classes: microRNAs (miRNAs), phased secondary small interfering RNAs (phasiRNA), and heterochromatic small interfering RNAs (hc-siRNA). miRNAs are 21 nt or 22 nt in size and are derived from a single strand Polymerase II (Pol II) transcript, with a characteristic hairpin folding structure. The miRNA precursor is typically processed into a mature miRNA duplex by a diverse set of proteins, including Dicer-like 1(DCL1) (Bologna & Voinnet, 2014; Li & Yu, 2021; Rogers & Chen, 2013). PhasiRNAs on the other hand are derived from a double strand Pol II and RNA-dependent RNA Polymerase VI (RDR6) transcript and are processed into 21-nt or 24-nt mature duplexes by DCL4 or DCL5. This dicing process is triggered by a 22 nt miRNA and results in consecutive phasing sRNAs (Fei et al., 2015). The third class of sRNAs, hc-siRNAs, are derived from repetitive regions of the genome, and are typically 24 nt in size.

In this article, we characterized sRNA accumulation in leaf, root, tuber, and flower tissues of potato cultivars Desiree and Eva, which were selected to capture a maximum diversity of sRNAs from vegetative and reproductive tissues.

2 | METHODS

2.1 | Plant materials

Desiree and Eva potatoes used in this study were from United States seed growers. Tuber RNA was extracted directly from seed tubers received from growers. To obtain root, leaf, and flower RNA, both cultivars were grown in a room at 16 h light and $22 \pm 3°C$ temperature. Leaf and root RNA was extracted from 6-week-old plants, whereas flower RNA was isolated at flowering.

2.2 | RNA extraction

Total RNA from leaves, flowers, and roots was extracted from three biological replicates of ground plant tissue TRIreagent (Ambion), following manufacturer's recommendations. Correspondingly, total RNA from tuber was isolated using the RNeasy Mini kit (Qiagen, USA) following manufacturer's recommendations, except using a modified tuber extraction buffer (6 M guanidine hydrochloride, 20 mM MES hydrate, 20 mM EDTA, pH 8, 10% b-mecaptoethanol). Quality and quantity of the extracted RNA was measured by running an RNA denaturing agarose gel, and qubit fluorometer assay.

2.3 | Annotation of potato genome

The RH genome assembly (Zhou et al., 2020) was downloaded from Spud DB (http://solanaceae.plantbiology.msu.edu/rh_potato_download.shtml). Based on this genome, repetitive regions, rRNAs, and tRNAs were annotated using computational software. Repetitive regions were annotated by RepeatMasker (http://www.repeatmasker.org), using the Viridiplantae database, whereas rRNA genes were predicted by RNAMMER (Lagesen et al., 2007), using default parameters. tRNAs genes were predicted by tRNAscan-SE 2.0 (Chan et al., 2021), using default parameters. All the final annotations produced by these software are available in the supporting information in gtf format.

2.4 | sRNA library preparation, sequencing, and analysis

Small RNA libraries were generated using Somagenics RealSeq®-AC miRNA Library Kit according to the manufacturer's protocol using barcodes. Libraries were pooled and sequenced using Illumina NextSeq 550 single end sequencing at the University of Delaware DNA Sequencing & Genotyping Center (Newark, DE, USA). Sequencing adapters were removed using cutadapt (Martin, 2011), retaining all reads between 18 and 34 nt in length without undetermined bases (cutadapt - a TGGAATTCTCGGGTGCCAAGG - m 18 - M 34 - j 0 -- max-n 0 -o sample.fastq). The quality of reads was assessed using FASTQC (https://www.bioinformatics.babraham.ac.uk/projects/fastqc/). Resulting reads were aligned to the RH potato genome (Zhou et al., 2020) and different features identified using bowtie2 (Langmead & Salzberg, 2013). miRNAs and phasiRNAs were identified from each cultivar separately using ShortStack version 3.8.5 (Axtell, 2013) with default parameters. We used Bedtools (Quinlan & Hall, 2010) intersect to identify predicted *PHAS* loci clusters located in coding regions, and BLAST (Altschul et al., 1990) alignment to discard *PHAS* loci clusters that contained sequences that aligned repetitive sequences and rRNA genes. miRNAs and phasiRNAs were manually curated based on their accumulation and structure. Previously annotated miRNAs for 10 species of plants were downloaded from miRbase v22 (Kozomara & Griffiths-Jones, 2014). To identify known miRNAs, we conducted a BLAST (Altschul et al., 1990) search using

the ShortStack predicted miRNA from ShortStack categories Y and N15 as a query, and the merged list of annotated miRNAs as the subject. Differential accumulation of miRNAs was done using DeSeq2 (Love et al., 2014) and raw counts resulting from Bowtie2 mapping. We set the false discovery rate (FDR) to 5%. miRNA target prediction was done using psRNATarget (Dai et al., 2018). General mapping statistics are included in Table S1.

3 | RESULTS

3.1 | Potato genome annotation

To understand the genomic origin of small RNAs in potato, we annotated common features, including ribosomal RNAs (rRNAs), transfer RNAs (tRNAs) and repetitive elements (Figure S2A) in the potato RH-89 genome. For rRNAs, we obtained 9292 genes corresponding to 8003 5.8S, 663 18S, and 626 28S. We also annotated 2555 tRNAs, representing all 22 amino acids, which corresponded to 55 out of the 64 codons (Figure S2A,B). We further found that 41.73% of the genome consisted of repetitive elements, where 37.13% were retroelements and 4.29% were DNA transposons

(Figure S2A,C). A vast majority of retroelements belonged to the long-terminal repeat (LTR) Gypsy family, followed in abundance by the LTR Copia family. This is consistent with previous studies done in Solanaceae (Baldrich et al., 2021; Galindo-González et al., 2017). While acknowledging that this analysis is likely not exhaustive, we note that due to the repetitiveness of these features, the study is sufficient to identify the sRNAs that originate from transposable elements.

3.2 | Potato tubers have a unique small RNA profile

In this study, we prepared sRNA libraries from leaves, roots, tubers, and flowers (pooled from different stages of plant development), and independently collected three biological replicates from three different plants for each cultivar and each tissue, for a total of 24 samples. Results of sequence analysis showed that in both potato cultivars, the size distribution of sRNAs of flower, leaf, and root tissues between 18 nt and 34 nt peaked at 24 nt, with a secondary peak at 21 nt, consistent with most other plant species (Figure 1). In contrast, tubers exhibited a unique sRNA profile, displaying a more uniform size
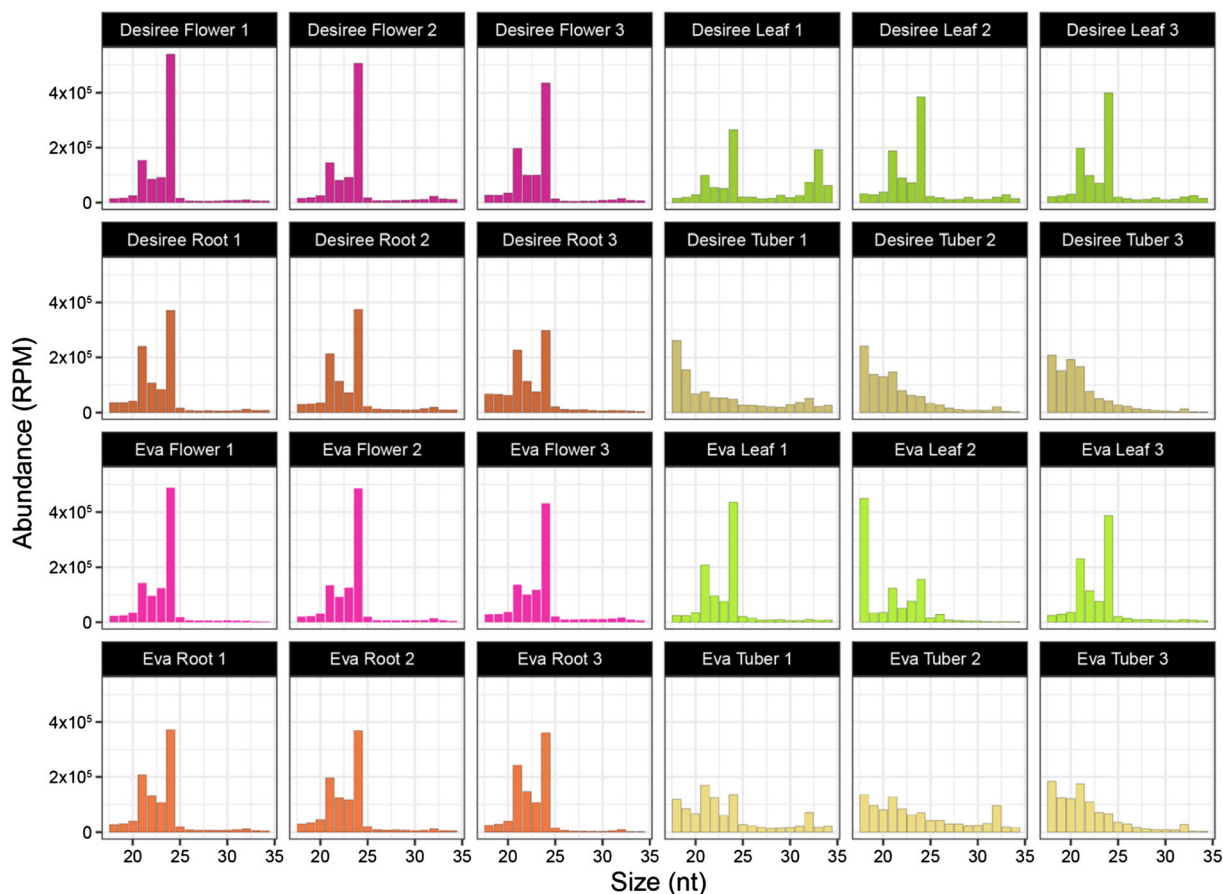

FIGURE 1 Size distribution of sRNAs mapping to the RH89 potato genome. For each of the samples, the abundance of each size class was calculated in reads per million (RPM). The x axis indicates the sRNA size, ranging from 18 to 34 nucleotides (nt), and the y axis indicates its abundance (RPM).

distribution with a partial peak at 21 nt (Figure 1). We observed that the 18 and 19 nt sRNAs from tubers originate from rRNAs and repetitive regions, with a small proportion originating from tRNAs (Figure S3). To determine the heterogenicity and size of each sequence, we analyzed the size distribution of distinct sRNA sequences, where each sequence is counted only once. Similar to total sRNA size distribution, we observed that flower, leaf, and root tissues displayed a predominant peak at 24 nt, usually corresponding to sRNAs from repetitive regions (Figure S4). Consistent with total sRNAs distribution recorded above, the distinct sRNAs peak at 24 nt was less predominant compared with secondary peaks at 21 and 22 nt, respectively. We also observed that the total count of distinct sRNA sequences was 10 times lower in tubers (19.4%) than in other tissues (46.4%) (Table S1).

3.3 | microRNAs and their accumulation are conserved between Desiree and Eva potato cultivars

To date, 343 mature potato miRNAs have been reported in miRbase (Kozomara et al., 2019). We used the sRNA data generated from Desiree and Eva potato cultivars to identify known and potentially novel potato miRNAs, using the ShortStack pipeline (Axtell, 2013; Johnson et al., 2016) with default parameters and obtained 112 MIR genes in Desiree and 109 MIR genes in Eva. We merged these two outputs and obtained a total of 160 MIR genes, 62 of which were identified in both cultivars. Of these 160 miRNA precursors, 128 were already annotated in miRBase v21 (Kozomara & Griffiths-Jones, 2014), and 32 are potential new miRNA candidates in potato. All observed miRNAs were expressed in at least one variety or tissue. Of these,
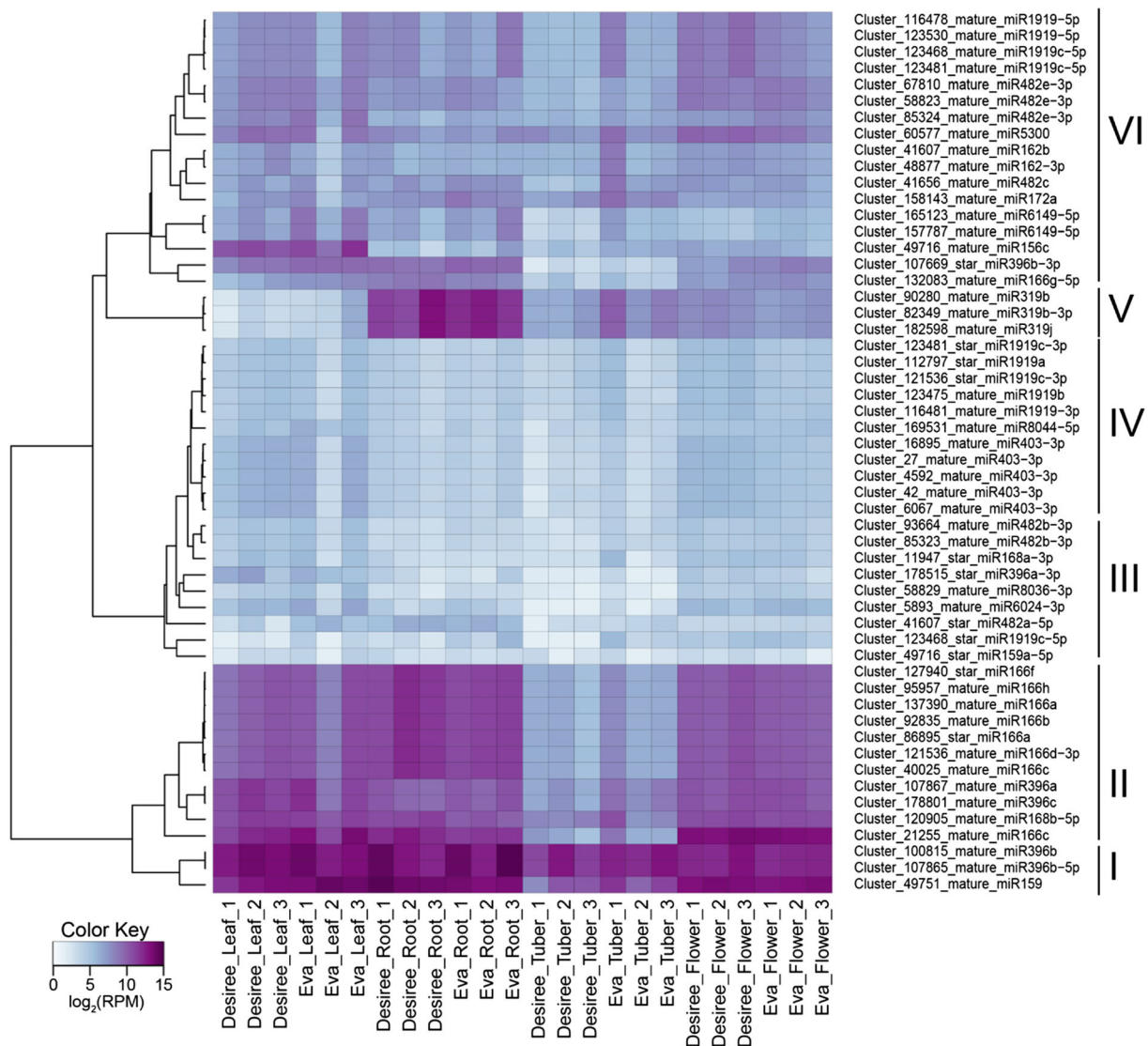

FIGURE 2 microRNAs and their accumulation are conserved between cultivars. For each sample, miRNA accumulation is represented as a heatmap, where white and light blue represent low accumulation and dark-blue and purple represent high accumulation. We only represent annotated miRNAs that accumulate in all tissues with at least 10 reads per million (RPM). miRNAs with a similar accumulation pattern are clustered together in six distinct clusters, labeled I to VI.

13 mature miRNAs accumulated only in Desiree and nine only in Eva (Tables S2 and S3).

To study miRNA tissue specificity, and avoid false negatives, we focused on those annotated miRNAs that accumulate in all tissues with at least 10 reads per million (RPM) (Figure 2). Three of these miR-NAs were expressed in all tissues at a high level, two of which are members of the miR396 family and the other a member of the miR159 family (Cluster I). We also observed that 11 miRNAs from families miR166, miR168 and miR396 (Cluster II) accumulated in all tissues at a high level, except in tubers. Accordingly, 11 miRNAs belonging to families miR1919, miR8044 and miR403 in cluster IV accumulated at higher levels in leaves and flowers but not in roots and tubers. Finally, the three miRNAs belonging to miR319 family in cluster V accumulated at high levels in flowers, but not in the other tissues.

To determine whether some of these miRNAs exhibit a difference in either of the two cultivars (Figure 3), we analyzed the differential accumulation of each miRNA in each tissue for both cultivars. A total of 44 miRNAs differentially accumulated in at least one of the tissues, 27 of which were previously annotated in miRBase and 17 potential novel miRNAs. In general, most of the differentially accumulated miR-NAs showed a lower accumulation in Desiree tissues compared with Eva (blue shades in Figure 3). Notably, miRNAs in families miR6149

and miR1919 showed a lower accumulation in several Desiree tissues compared with Eva. In contrast, miRNAs from families miR403, miR530, and miR170 showed a higher accumulation in Desiree tissues than in Eva tissues (orange shades in Figure 3).

3.4 | PhasiRNA have a similar expression in both potato cultivars

Using the same output generated by ShortStack, we identified pha-siRNAs in both cultivars separately and obtained 161 21-nt *PHAS* and 45 24-nt *PHAS* loci in Eva, as well as 142 21-nt *PHAS* and 75 24-nt *PHAS* loci in Desiree. Of these, we focused on the *PHAS* loci that were common to both cultivars, corresponding to 61 21-nt *PHAS* from coding regions, 39 21-nt *PHAS* from noncoding regions; nine 24-nt *PHAS* from coding regions, and 11 24-nt *PHAS* from non-coding regions of the genome. To analyze the expression of each of these *PHAS* loci, heatmaps for all four *PHAS* categories were gener-ated. Results showed that among the 21-nt *PHAS* loci that over-lapped with coding genes (Figure 4a), 25 were disease resistance genes, five were kinases, and one was DCL2, consistent with previ-ous reports for other plant species (Baldrich et al., 2021; Fei et al., 2015; Reyes-Chin-Wo et al., 2017). We also observed a
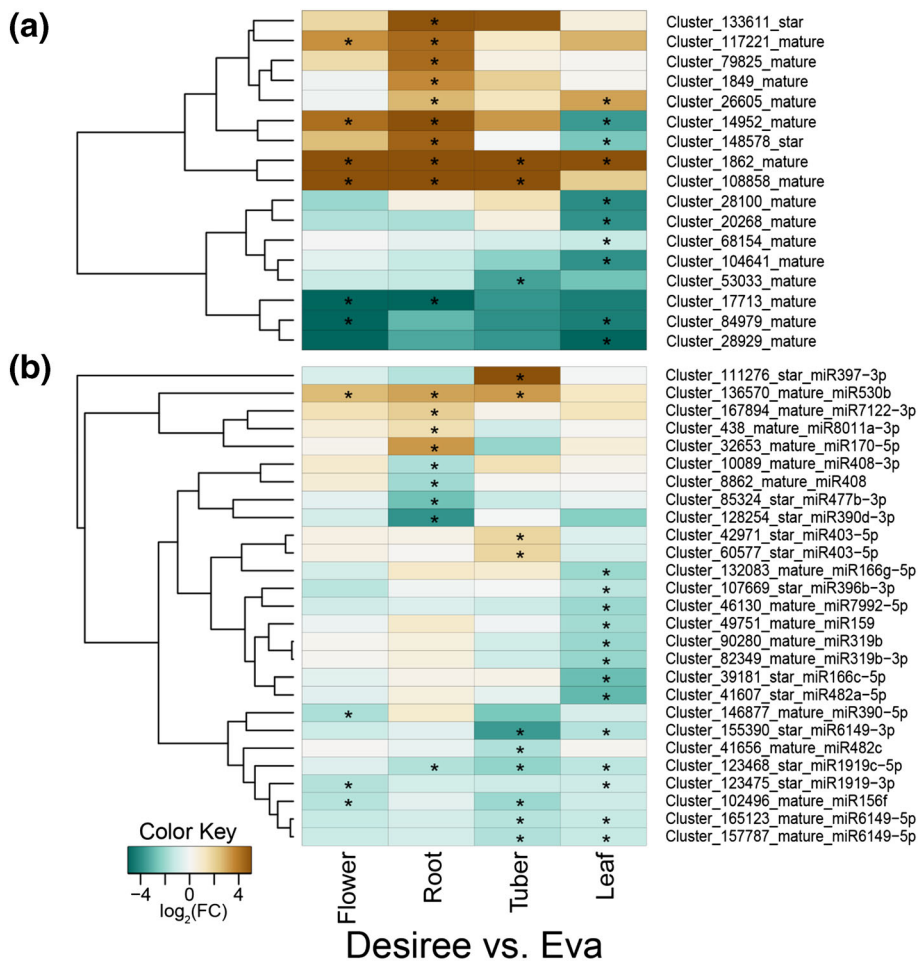

FIGURE 3 The microRNAs that have a differential accumulation between cultivars are mostly tissue specific. For each tissue, flower, root, tuber and leaf, differential miRNA accumulation is represented as a heatmap, where blue represents low accumulation in Desiree compared with Eva, and dark orange represents high accumulation in Desiree compared with Eva. The asterisks represent significant differential expression, with a *p*-value of .05 or lower. (a) miRNAs candidates; (b) annotated miRNAs
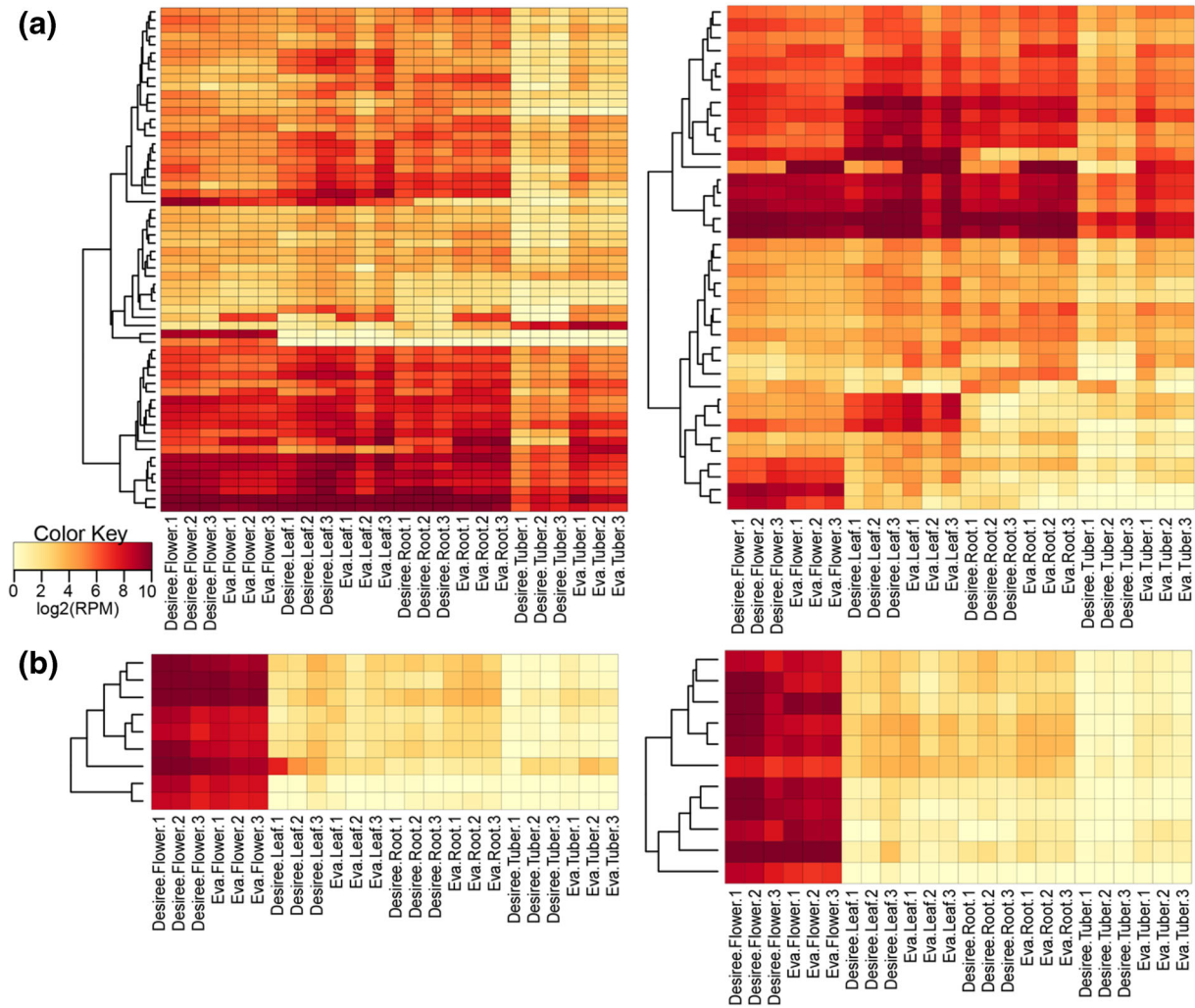
FIGURE 4 PhasiRNAs have a similar expression in both cultivars. For each sample, *PHAS* locus accumulation is represented as a heatmap, where white and light yellow represent low accumulation and red represents high accumulation. Only *PHAS* loci that are present in both cultivars in logarithmic scale of reads per million (RPM) are represented. miRNAs with a similar accumulation pattern are clustered together. (a) 21-phasiRNA producing loci from coding (left panel) and noncoding (right panel) origin. (b) 24-phasiRNA producing loci from coding (left panel) and noncoding (right panel) origin.

cluster of 20 loci that are highly expressed in all tissues, as well as two that appear to be flower specific (RHC10H1G1729.2 - Basic chitinase and RHC08H2G1411.2 - Pectinacetylesterase), one tuber specific (RHC06H2G2216.2 - methyl-CPG-binding domain 10), and one that appears to have a higher expression in all Eva tissues (RHC04H1G0134.2 - unidentified function). As for the 21-nt *PHAS* loci from noncoding regions, four loci appear to show flower specific expression, three with leaf specific, and one with a higher expression in all Eva tissues compared with Desiree. All 24-nt *PHAS* loci were observed to display a flower specific expression (Figure 4b and Figure S5) and showed no significant difference between Eva and Desiree.

To identify the triggers of these *PHAS* loci, we carried out a reverse analysis of target prediction using the miRNAs and *PHAS* loci identified in this study. To avoid false positives, only 22-nt miRNAs were selected as potential triggers. This analysis identified putative triggers for 15 out of the 20 24-nt *PHAS* loci, and 43 out of the 100 21-nt *PHAS* loci. These triggers include miR477, miR482, miR828, miR3627, miR8036 (a member of the miR482 family), miR8050, miR4414, miR6024, miR7122, as well as two potential new miRNAs not found in miRBASe. Most of these miRNAs were previously identified in other studies as *PHAS* triggers in different species (Feng et al., 2019; Guan et al., 2014; Seo et al., 2018; Wu et al., 2017; Xia et al., 2013; Zhu et al., 2013) (Table S4).

3.5 | hc-siRNAs have a tissue-specific accumulation pattern

Here, we defined heterochromatic siRNAs (hc-siRNAs) as all small RNAs reads that originate from repetitive regions of the genome, as defined by RepeatMasker. More specifically, we focus on the

FIGURE 5 hc-siRNAs show a tissue specific accumulation pattern. For each tissue, hc-siRNA accumulation is represented as a bar plot, where each shade of blue represents a different biological replicate. The x axis indicates transposable element of origin, and the y axis indicates its abundance (RPM). The three shades of blue represent the three biological replicates for each sample type.
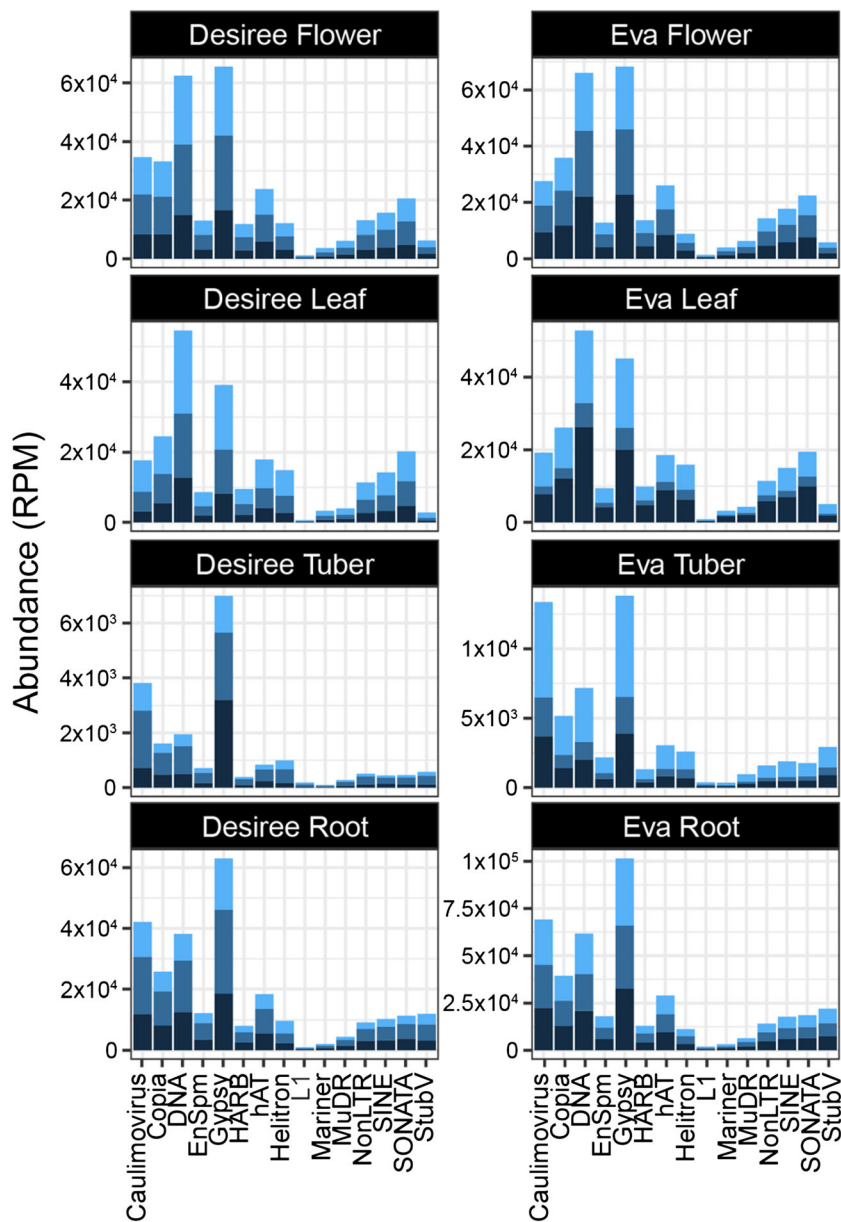
hc-siRNAs that derive from transposable elements (TEs). To determine tissue accumulation of hc-siRNAs, we first identified TEs, and then queried our data to quantify the number of sRNAs mapping each superfamily of TE (Figure 5). We observed that in both cultivars, each tissue presents a specific hc-siRNA origin and abundance. For example, in flowers and leaves, most of the hc-siRNAs originate from DNA and Gypsy elements, followed by Copia and endogenized caulimoviruses. However, in tubers and roots, the most abundant hc-siRNAs originate from Gypsy and endogenized caulimoviruses. Gypsy elements were the most abundant TE annotated in the genome (~30%; Figure S3); thus, there was a correlation between the number of TE and the number of sRNAs. However, caulimovirus sequences represented only 1.5% of the genome even though accounting for the second most abundant sRNAs. We note that sRNAs derived from endogenized viruses have been reported in potato (Geering et al., 2014); have been suggested to be involved in

virus defense (Niraula & Fondong, 2021) and may be a source of novel genetic material.

A size distribution analysis of hc-siRNAs derived from different TEs showed that reads originating from caulimovirus and StubV (a new type of endogenous florendovirus, (Geering et al., 2014) were mostly 22 nt long. In contrast, reads originating from Helitron elements were 21 nt long, whereas reads originating from all the other elements were mostly 24 nt long (Figure S6A).

4 | DISCUSSION

In this study, we analyze sRNA datasets from leaf, flower, root, and tuber tissues of commercial potato cultivars Eva and Desiree. This analysis found that only 6% of the miRNAs identified in our samples, corresponding to 21 out of 320, are apparently cultivar specific.

Additionally, these apparently cultivar-specific miRNAs that were previously annotated in miRBase have members from the same family present that should have the same targets. This, added to the fact that the accumulation of almost all miRNAs is conserved between both cultivars, suggests that the apparent cultivar-specific miRNAs are more an artifact than the result of a speciation. This leads us to conclude that all miRNAs that were identified in this study are conserved in both cultivars.

We also found that some miRNAs have a significantly different accumulation in both cultivars, these include miR397-3p, miR530, miR7122, miR170, and miR403. These miRNAs, which were more abundant in Desiree compared with Eva, have been found to be involved in plant responses to stress (Dong & Pei, 2014; Kohli et al., 2014; Li et al., 2021; Manacorda et al., 2021; Xia et al., 2013). Future research efforts would determine whether these miRNAs are responsible for some of the stress responsive differences between Desiree and Eva.

In these same datasets, we identified phasiRNAs originating from coding and noncoding RNAs and producing both 21-nt and 24-nt siRNAs. As reported previously in other Solanaceae species (Baldrich et al., 2021; Xia et al., 2019), all the identified 24-nt phasiRNAs from coding and noncoding genes, were found only in flowers. Furthermore, most 21-nt phasiRNAs from coding genes were observed to be from disease resistance genes and kinases. We hypothesize that this additional layer of regulation allows for fine-tuned expression, in which genes can be continuously transcriptionally active and regulated post-transcriptionally at the same time, allowing for a fast response when needed.

The main role of hc-siRNAs is to maintain genome integrity by regulating epigenetic modifications of repetitive elements. We previously reported that potato lacks hc-siRNAs, likely due to its mostly asexual reproduction nature (Baldrich et al., 2021). However, here, we observed that all potato tissues, except for tubers, produce a typical level of hc-siRNAs (Figure S6B). We postulate that this difference might be driven by the sampling bias of previous studies, mostly centered in tubers. To fully understand the connection between mode of reproduction and silencing pathways, future studies might be necessary to analyze hc-siRNAs in sexually and asexually reproducing potatoes.

Here, we also identified three types of hc-siRNAs, including 21 nt and originating from Helitrons, 22 nt and originating from integrated viral sequences, and 24 nt and originating from all other TEs. The presence of 21- and 22-nt hc-siRNAs from Helitron, caulimoviruses, and StubV, suggests that these endogenized genes might be transcriptionally active and their silencing is mediated by RDR6 and DCL2 (Fultz et al., 2015; Nuthikattu et al., 2013). In the future, it would be interesting to generate RNA-seq data from these tissues to determine whether these TEs are transcribed. It would also be interesting to analyze the accumulation of hc-siRNA in potato RDR and/or DCL mutants, to clarify the silencing pathway of each TE superfamily.

Together, data presented here show a complete sRNA atlas of miRNAs, phasiRNAs, and hc-siRNAs in four different tissues of two commercial potato cultivars. Our results support the hypothesis that the vast majority of sRNAs are not cultivar specific. However, their accumulation is different and might have some physiological implications that would need to be studied in future research efforts.

CONFLICTS OF INTEREST

The authors declare no conflicts of interest associated with the work described in this manuscript.

AUTHOR CONTRIBUTIONS

PB, VNF and BCM designed the experiments. AL generated the libraries. PB and AL analyzed the data. PB and VNF wrote the manuscript.

DATA AVAILABILITY STATEMENT

The data discussed in this publication have been deposited in NCBI's Gene Expression Omnibus (Edgar et al., 2002) and are accessible through GEO Series accession number GSE213986 (https://www.ncbi.nlm.nih.gov/geo/query/acc.cgi?acc=GSE213986).

ORCID

Patricia Baldrich https://orcid.org/0000-0003-4669-6632
Alexander Liu https://orcid.org/0000-0002-3836-6556
Blake C. Meyers https://orcid.org/0000-0003-3436-6097
Vincent N. Fondong https://orcid.org/0000-0002-3451-5200

REFERENCES

Altschul, S. F., Gish, W., Miller, W., Myers, E. W., & Lipman, D. J. (1990). Basic local alignment search tool. *Journal of Molecular Biology*, *215*(3), 403–410. https://doi.org/10.1016/S0022-2836(05)80360-2

Aversano, R., Contaldi, F., Ercolano, M. R., Grosso, V., Iorizzo, M., Tatino, F., Xumerle, L., Dal Molin, A., Avanzato, C., Ferrarini, A., Delledonne, M., Sanseverino, W., Cigliano, R. A., Capella-Gutierrez, S., Gabaldón, T., Frusciante, L., Bradeen, J. M., & Carputo, D. (2015). The Solanum commersonii Genome Sequence Provides Insights into Adaptation to Stress Conditions and Genome Evolution of Wild Potato Relatives. *The Plant Cell*, *27*(4), 954–968. https://doi.org/10.1105/tpc.114.135954

Axtell, M. J. (2013). ShortStack: Comprehensive annotation and quantification of small RNA genes. *RNA*, *19*(6), 740–751. https://doi.org/10.1261/rna.035279.112

Baldrich, P., Bélanger, S., Kong, S., Pokhrel, S., & Tamim, S. (2021). "The Evolutionary History of Small RNAs in the Solanaceae." bioRxiv. https://www.biorxiv.org/content/10.1101/2021.05.26.445884.abstract

Baldrich, P., Beric, A., & Meyers, B. C. (2018). Despacito: the slow evolutionary changes in plant microRNAs. *Current Opinion in Plant Biology*, *42*, 16–22. https://doi.org/10.1016/j.pbi.2018.01.007

Bologna, N. G., & Voinnet, O. (2014). The diversity, biogenesis, and activities of endogenous silencing small RNAs in Arabidopsis. *Annual Review of Plant Biology*, *65*, 473–503. https://doi.org/10.1146/annurev-arplant-050213-035728

Chan, P. P., Lin, B. Y., Mak, A. J., & Lowe, T. M. (2021). tRNAscan-SE 2.0: improved detection and functional classification of transfer RNA genes. *Nucleic Acids Research*, *49*(16), 9077–9096. https://doi.org/10.1093/nar/gkab688

Dai, X., Zhuang, Z., & Zhao, P. X. (2018). psRNATarget: A plant small RNA target analysis server (2017 release). *Nucleic Acids Research*, *46*(W1), W49–W54.

Dong, C.-H., & Pei, H. (2014). Over-expression of miR397 improves plant tolerance to cold stress in Arabidopsis Thaliana. *Journal of Plant Biology = Singmul Hakhoe Chi*, *57*(4), 209–217. https://doi.org/10.1007/s12374-013-0490-y

Edgar, R., Domrachev, M., & Lash, A. E. (2002). Gene Expression Omnibus: NCBI gene expression and hybridization array data repository. *Nucleic Acids Research*, *30*(1), 207–210. https://doi.org/10.1093/nar/30.1.207

Fei, Q., Li, P., Teng, C., & Meyers, B. C. (2015). Secondary siRNAs from Medicago NB-LRRs modulated via miRNA-target interactions and their abundances. *The Plant Journal: For Cell and Molecular Biology*, *83*(3), 451–465. https://doi.org/10.1111/tpj.12900

Feng, L., Xia, R., & Liu, Y. (2019). Comprehensive characterization of miRNA and *PHAS* loci in the diploid strawberry (Fragaria Vesca) genome. *Horticultural Plant Journal*, *5*(6), 255–267. https://doi.org/10.1016/j.hpj.2019.11.004

Fultz, D., Choudury, S. G., & Slotkin, R. K. (2015). Silencing of active transposable elements in plants. *Current Opinion in Plant Biology*, *27*(October), 67–76. https://doi.org/10.1016/j.pbi.2015.05.027

Galindo-González, L., Mhiri, C., Deyholos, M. K., & Grandbastien, M.-A. (2017). LTR-retrotransposons in plants: Engines of Evolution. *Gene*, *626*(August), 14–25. https://doi.org/10.1016/j.gene.2017.04.051

Geering, A. D. W., Maumus, F., Copetti, D., Choisne, N., Zwickl, D. J., Zytnicki, M., McTaggart, A. R., Scalabrin, S., Vezzulli, S., Wing, R. A., Quesneville, H., & Teycheney, P.-Y. (2014). Endogenous Florendoviruses are major components of plant genomes and hallmarks of virus evolution. *Nature Communications*, *5*(November), 5269. https://doi.org/10.1038/ncomms6269

Guan, X., Pang, M., Nah, G., Shi, X., Ye, W., Stelly, D. M., & Jeffrey Chen, Z. (2014). miR828 and miR858 regulate Homoeologous MYB2 gene functions in Arabidopsis Trichome and cotton fibre development. *Nature Communications*, *5*(1), 1, 3050–14. https://doi.org/10.1038/ncomms4050

Johnson, N. R., Yeoh, J. M., Coruh, C., & Axtell, M. J. (2016). Improved Placement of Multi-mapping Small RNAs. *G3 (Bethesda, Md.)*, *6*(7), 2103–2111. https://doi.org/10.1534/g3.116.030452

Jones, R. A. C., & Vincent, S. J. (2018). Strain-specific hypersensitive and extreme resistance phenotypes elicited by potato virus Y among 39 potato cultivars released in three world regions over a 117-year period. *Plant Disease*, *102*(1), 185–196. https://doi.org/10.1094/PDIS-06-17-0901-RE

Kohli, D., Joshi, G., Deokar, A. A., Bhardwaj, A. R., Agarwal, M., Katiyar-Agarwal, S., Srinivasan, R., & Jain, P. K. (2014). Identification and characterization of wilt and salt stress-responsive microRNAs in chickpea through high-throughput sequencing. *PLoS ONE*, *9*(10), e108851. https://doi.org/10.1371/journal.pone.0108851

Kozomara, A., & Griffiths-Jones, S. (2014). miRBase: Annotating high confidence microRNAs using deep sequencing data. *Nucleic Acids Research*, *42*, 68–73. https://doi.org/10.1093/nar/gkt1181

Kozomara, A., Birgaoanu, M., & Griffiths-Jones, S. (2019). miRBase: from microRNA sequences to function. *Nucleic Acids Research*, *47*(D1), D155–D162. https://doi.org/10.1093/nar/gky1141

Kyriakidou, M., Anglin, N. L., Ellis, D., Tai, H. H., & Strömvik, M. V. (2020). Genome assembly of six Polyploid potato genomes. *Scientific Data*, *7*(1), 88. https://doi.org/10.1038/s41597-020-0428-4

Lagesen, K., Hallin, P., Rødland, E. A., Staerfeldt, H. H., Rognes, T., & Ussery, D. W. (2007). RNAmmer: consistent and rapid annotation of ribosomal RNA genes. *Nucleic Acids Research*, *35*(9), 3100–3108. https://doi.org/10.1093/nar/gkm160

Langmead, B., & Salzberg, S. L. (2013). Langmead. 2013. Bowtie2. *Nature Methods*, *9*, 357–359. https://doi.org/10.1038/nmeth.1923

Leisner, C. P., Hamilton, J. P., Crisovan, E., Manrique-Carpintero, N. C., Marand, A. P., Newton, L., Pham, G. M., Jiang, J., Douches, D. S., Jansky, S. H., & Buell, C. R. (2018). Genome sequence of M6, a diploid inbred clone of the high-glycoalkaloid-producing tuber-bearing potato species Solanum chacoense, reveals residual heterozygosity. *The Plant Journal: For Cell and Molecular Biology*, *94*(3), 562–570. https://doi.org/10.1111/tpj.13857

Li, M., & Yu, B. (2021). Recent advances in the regulation of plant miRNA biogenesis. *RNA Biology*, *18*(12), 2087–2096. https://doi.org/10.1080/15476286.2021.1899491

Li, Y., Wang, L.-F., Bhutto, S. H., He, X.-R., Yang, X.-M., Zhou, X.-H., Lin, X.-Y., Rajput, A. A., Li, G.-B., Zhao, J.-H., Zhou, S.-X., Ji, Y.-P., Pu, M., Wang, H., Zhao, Z.-X., Huang, Y.-Y., Zhang, J.-W., Qin, P., Fan, J., & Wang, W.-M. (2021). Blocking miR530 improves Rice resistance, yield, and maturity. *Frontiers in Plant Science*, *12*(August), 729560. https://doi.org/10.3389/fpls.2021.729560

Love, M. I., Huber, W., & Anders, S. (2014). Moderated estimation of fold change and dispersion for RNA-Seq data with DESeq2. *Genome Biology*, *15*(12), 1, 550–21. https://doi.org/10.1186/s13059-014-0550-8

Machida-Hirano, R. (2015). Diversity of potato genetic resources. *Breeding Science*, *65*(1), 26–40. https://doi.org/10.1270/jsbbs.65.26

Manacorda, C. A., Tasselli, S., Marano, M. R., & Asurmendi, S. (2021). "TuMV infection alters miR168/AGO1 and miR403/AGO2 systems regulation in Arabidopsis." *bioRxiv*. https://doi.org/10.1101/2021.02.17.431672

Martin, M. (2011). Cutadapt removes adapter sequences from high-throughput sequencing reads. *EMBnet Journal*, *17*, 10–12. https://doi.org/10.14806/ej.17.1.200

Niraula, P. M., & Fondong, V. N. (2021). Development and adoption of genetically engineered plants for virus resistance: Advances, opportunities and challenges. *Plants*, *10*(11), 2339. https://doi.org/10.3390/plants10112339

Nuthikattu, S., McCue, A. D., Panda, K., Fultz, D., DeFraia, C., Thomas, E. N., & Keith Slotkin, R. (2013). The initiation of epigenetic silencing of active transposable elements is triggered by RDR6 and 21-22 nucleotide small interfering RNAs. *Plant Physiology*, *162*(1), 116–131. https://doi.org/10.1104/pp.113.216481

Plaisted, R. L., Halseth, D. E., Brodie, B. B., Slack, S. A., Sieczka, J. B., Christ, B. J., Paddock, K. M., & Peck, M. W. (2001). Eva:A midseason Golden nematode- and virus-resistant variety for use as Tablestock or Chipstock. *American Journal of Potato Research: An Official Publication of the Potato Association of America*, *78*(1), 65–68. https://doi.org/10.1007/BF02874826

Quinlan, A. R., & Hall, I. M. (2010). BEDTools: A flexible suite of Utilities for Comparing Genomic Features. *Bioinformatics*, *26*(6), 841–842. https://doi.org/10.1093/bioinformatics/btq033

Reyes-Chin-Wo, S., Wang, Z., Yang, X., Kozik, A., Arikit, S., Song, C., Xia, L., Froenicke, L., Lavelle, D. O., Truco, M.-J., Xia, R., Zhu, S., Xu, C., Xu, H., Xu, X., Cox, K., Korf, I., Meyers, B. C., & Michelmore, R. W. (2017). Genome assembly with in vitro proximity ligation data and whole-genome triplication in lettuce. *Nature Communications*, *8*(April), 14953. https://doi.org/10.1038/ncomms14953

Rogers, K., & Chen, X. (2013). Biogenesis, turnover, and mode of action of plant microRNAs. *The Plant Cell*, *25*(7), 2383–2399. https://doi.org/10.1105/tpc.113.113159

Samad, A. F. A., Nazaruddin, N., Sajad, M., Jani, J., Murad, A. M. A., Zainal, Z., & Ismail, I. (2017). Small RNA sequencing for secondary metabolite analysis in *Persicaria minor*. *Genomics Data*, *13*, 3–4. https://doi.org/10.1016/j.gdata.2017.05.014

Seo, E., Kim, T., Park, J. H., Yeom, S.-I., Kim, S., Seo, M.-K., Shin, C., & Choi, D. (2018). Genome-wide comparative analysis in Solanaceous species reveals evolution of microRNAs targeting defense genes in capsicum Spp. *DNA Research: An International Journal for Rapid Publication of Reports on Genes and Genomes*, *25*(6), 561–575. https://doi.org/10.1093/dnares/dsy025

Tiwari, J. K., Buckseth, T., Zinta, R., Bhatia, N., Dalamu, D., Naik, S., Poonia, A. K., Kardile, H. B., Challam, C., Singh, R. K., Luthra, S. K., Kumar, V., & Kumar, M. (2022). Germplasm, breeding, and genomics in potato improvement of biotic and abiotic stresses tolerance. *Frontiers in Plant Science*, *13*(February), 805671. https://doi.org/10.3389/fpls.2022.805671

Watanabe, K. (2015). Potato genetics, genomics, and applications. *Breeding Science*, *65*(1), 53–68. https://doi.org/10.1270/jsbbs.65.53

Wu, F., Chen, Y., Tian, X., Zhu, X., & Jin, W. (2017). Genome-wide identification and characterization of phased small interfering RNA genes in response to botrytis Cinerea infection in solanum Lycopersicum. *Scientific Reports*, *7*(1), 3019. https://doi.org/10.1038/s41598-017-02233-x

Xia, R., Chen, C., Pokhrel, S., Ma, W., Huang, K., Patel, P., Wang, F., Xu, J., Liu, Z., Li, J., & Meyers, B. C. (2019). 24-Nt reproductive phasiRNAs are broadly present in angiosperms. *Nature Communications*, *10*(1), 627. https://doi.org/10.1038/s41467-019-08543-0

Xia, R., Meyers, B. C., Liu, Z., Beers, E. P., Ye, S., & Liu, Z. (2013). MicroRNA Superfamilies descended from miR390 and their roles in secondary small interfering RNA biogenesis in eudicots. *The Plant Cell*, *25*(5), 1555–1572. https://doi.org/10.1105/tpc.113.110957

Xu, X., Pan, S., Cheng, S., Zhang, B., Mu, D., Ni, P., Zhang, G., Yang, S., Li, R., Wang, J., Orjeda, G., Guzman, F., Torres, M., Lozano, R., Ponce, O., Martinez, D., De la Cruz, G., Chakrabarti, S. K., Patil, V. U., … Potato Genome Sequencing Consortium. (2011). Genome sequence and analysis of the tuber crop potato. *Nature*, *475*(7355), 189–194. https://doi.org/10.1038/nature10158

Zhou, Q., Tang, D., Huang, W., Yang, Z., Zhang, Y., Hamilton, J. P., Visser, R. G. F., Bachem, C. W. B., Robin Buell, C., Zhang, Z., Zhang, C., & Huang, S. (2020). Haplotype-resolved genome analyses of a heterozygous diploid potato. *Nature Genetics*, *52*(10), 1018–1023. https://doi.org/10.1038/s41588-020-0699-x

Zhu, Q.-H., Fan, L., Liu, Y., Xu, H., Llewellyn, D., & Wilson, I. (2013). miR482 regulation of NBS-LRR defense genes during fungal pathogen infection in cotton. *PloS One*, *8*(12), e84390.

SUPPORTING INFORMATION

Additional supporting information can be found online in the Supporting Information section at the end of this article.